Prediction of Crack Propagation in Large-Area Sintered Ag Joints for Bonding Power Modules and Coolers in Electric Vehicle Inverters

Tomoya Kazumi, Shinya Yano, Kenta Emori
Nissan Motor Co., Ltd
Yokosuka, Kanagawa, Japan
Ph: +81 70-3337-9843;
Email: t-kazumi@mail.nissan.co.jp

Abstract

Sintered Ag Joints are promising technology that significantly reduces thermal resistance compared to conventional solder joints and have been widely applied to chip-level and small-package interfaces. However, their application to large-area interfaces in electric vehicle (EV) inverters remains limited due to reliability issues associated with thermally induced stresses, which lead to crack propagation and performance degradation. This study proposes a design-oriented crack-propagation prediction methodology for large-area sintered Ag joints used in power module–to–cooler bonding. Large-area joint samples (53 mm × 42 mm), consisting of a power module bonded to a metal plate, were fabricated and subjected to temperature cycling tests. Crack propagation behavior was experimentally evaluated using scanning acoustic tomography, and lifetime was defined as the number of cycles required for a crack length corresponding to a specified increase in thermal resistance. Finite element analysis was conducted to calculate thermally induced strain, and the strain amplitude, including plastic and creep components, was used as the crack-driving parameter. A strong correlation between strain amplitude and crack-propagation lifetime was obtained, and a Coffin–Manson-type model with a high coefficient of determination ($R^2 > 0.97$) was established. Based on this model, three inverter cooler structures were designed to reduce strain amplitude. Prototype evaluations confirmed that reducing strain amplitude effectively suppresses crack propagation. The proposed methodology enables quantitative lifetime prediction and provides practical design guidelines for improving the reliability of large-area sintered Ag joints in EV inverter applications.

Key words

Sintered Ag Joint, Large Area, Crack Propagation, Lifetime Prediction, EV Inverter, Power Modules

I. Introduction

As EVs advance toward higher power-density operation, the heat density in inverters increases significantly, making effective cooling structures increasingly important [1].

An inverter cooling structure typically consists of power modules that contain power semiconductor chips, thermal interface materials (TIMs), and a cooler [2]. Conventionally, solders have been used as TIMs to directly bond these components [3]. However, the thermal conductivity of typical solders is more than one order of magnitude lower than that of aluminum or copper, which constitute the main parts of the cooling structure, and thus the solder layer remains a major bottleneck in reducing the thermal resistance from semiconductor chips to the coolant [4], [5]. In addition, wide-bandgap semiconductors such as SiC and GaN, which are increasingly adopted in EV inverters, can operate at junction temperatures exceeding 250 °C, whereas the melting point of most solders is around 200 °C, imposing fundamental limitations on their applicability [6], [7].

To address these challenges, sintered Ag joints, which bond nano- or microparticle Ag pastes under pressure and heat, have attracted significant attention [8]. Silver exhibits the highest thermal conductivity among metals and can be sintered well below its melting point, offering both low thermal resistance and high heat resistance. As a result, sintered Ag joints have already been applied to small-area interconnections on the order of a few millimeters, such as chip-to-substrate bonding in power modules [9].

In contrast, the application of sintered Ag joints to large-area interfaces on the order of several tens of millimeters, such as power module-to-cooler interfaces, remains limited because during temperature changes, large-area joints experience substantial three-dimensional thermal stresses, which promote crack initiation and

propagation within the sintered Ag layer [10]. Furthermore, the failure behavior of sintered Ag differs from that of conventional solders owing to its distinct elastoplastic and creep characteristics. Long-term reliability is influenced by multiple structural parameters, including material properties, layer thicknesses, and component dimensions. However, design guidelines that systematically relate bonding structure, thermally induced stress, and crack propagation behavior in large-area sintered Ag joints have not yet been established. Consequently, extensive prototyping and repetitive reliability testing are still required, leading to increased development cost and time.

The objective of this study is to establish a design-oriented crack-propagation prediction methodology for large-area sintered Ag joints used in power module-to-cooler bonding. Power modules were bonded to metal plates to fabricate large-area sintered Ag joint samples, and temperature cycling tests (TCTs) were performed to experimentally evaluate crack-propagation behavior. Thermally induced stresses and strains in the joint layer were analyzed using finite element analysis (FEA), and the analytical results were correlated with experimental observations to develop a crack-propagation prediction model. Finally, the proposed model was applied to the design of prototype bonding structures for an actual EV inverter configuration.

II. Experimental Method

A. Joint samples

Large-area sintered Ag joint samples were fabricated by bonding a SiC power module (TRCDRIVE pack, ROHM Co., Ltd.) on the upper side and a metal plate representing a cooler on the lower side using a commercially Ag sintering paste (ALPHA Argomax 2047, MacDermid Performance Solutions), as shown in Fig. 1. The bonding area was 53 mm × 42 mm. After stencil printing the Ag paste through a metal mask, the samples were sintered at 250 °C under a pressure of 15 MPa for 15 minutes in an atmospheric environment.

To systematically investigate the influence of structural parameters on thermomechanical behavior, nine types of joint samples were prepared by varying the upper side, lower side, the thickness of the metal plate, thickness of the sintered Ag layer and the temperature cycling conditions. The detailed sample configurations are summarized in Table 1.

B. Crack propagation evaluation in TCTs

The fabricated joint samples were subjected to TCTs to evaluate crack propagation behavior under thermomechanical loading. TCTs were conducted under two conditions: −40 °C to 120 °C and −60 °C to 175 °C with a dwell time of 15 minutes at each temperature. During these tests, thermally induced stress caused cyclic deformation in the sintered Ag layer. Crack propagation behavior was evaluated at predetermined cycle counts (100, 250, 500, and 1000 cycles) using scanning acoustic tomography (SAT). The observations revealed that the joint was initially intact across the entire bonding area, whereas cracks initiated at the corners and propagated inward with increasing cycle count as shown in Fig. 2.

In this study, the lifetime was defined as the number of cycles required for a crack to propagate 8 mm from the corner of the joint. This definition is based on thermal analysis results showing that a crack length of 8 mm corresponds to approximately a 20% increase in thermal resistance. Such a criterion is widely used as a practical failure threshold based on AQG-324 for automotive power module reliability evaluations.

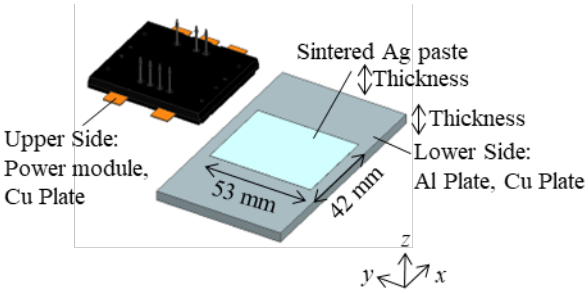


Figure 1. Schematic illustration of the large-area sintered Ag joint samples

Table 1 The detailed joint sample configurations

	No.1	No.2	No.3	No.4	No.5	No.6	No.7	No.8	No.9
Upper side	Power Module	Power Module	Power Module	Power Module	Power Module	Cu plate	Power Module	Power Module	Power Module
Lower side	Al plate	Al plate	Al plate	Al plate	Al plate	Al plate	Al plate	Al plate	Cu plate
Thickness of metal plate [mm]	10	10	5	5	2.5	5	5	5	5
Thickness of Sintered Ag [μm]	50	100	50	100	100	100	50	100	100
Temperature cycle [°C]	-40 120	-40 120	-40 120	-40 120	-40 120	-40 120	-60 175	-60 175	-60 175

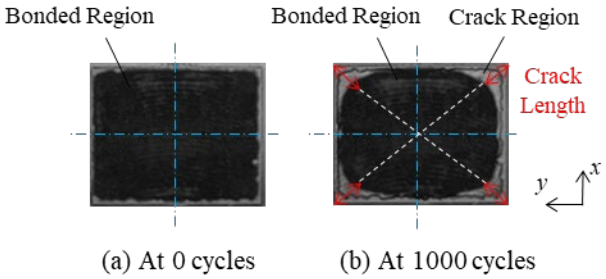


Figure 2. Crack propagation behavior of sample No.4 evaluated by SAT: (a) 0 cycles and (b) 1000 cycles.

III. Analytical Method

A. Finite element analysis models

Thermomechanical behavior during TCTs was analyzed using non-linear FEA performed with Abaqus (Dassault Systèmes). Owing to geometric symmetry in both the *x* and *y* directions, a quarter-symmetric three-dimensional model was employed to reduce computational cost while maintaining accuracy shown in Fig. 3(a) and (b). To further improve computational efficiency without compromising accuracy, the power module was simplified by modeling only the mold resin and insulating substrate, while components such as chips and busbars were omitted.

A tetrahedral mesh was used for the entire model shown in Fig.3(c), and local mesh refinement was applied in the corner regions of the sintered Ag layer, where crack initiation and propagation were expected due to stress concentration.

Strain evaluation was conducted within an arc-shaped region corresponding to an 8 mm crack as shown in Fig. 3(d), enabling direct comparison with the experimentally defined failure criterion.

A cross-sectional view of the model is shown in Fig. 3(e). The material properties of each component are listed in Table 2. The elastoplastic and creep properties of the sintered Ag were obtained from three-point bending tests shown in Fig.4, which were conducted over a temperature range of 20 °C to 200 °C, whereas those of the other materials were taken from the material database [11].

B. Strain amplitude

The strain amplitude was selected as the crack-driving parameter because crack propagation in sintered Ag is governed by cyclic plastic deformation and creep strain accumulation under thermal loading [12],[13]. The strain amplitude $\Delta\varepsilon$, was defined as half of the sum of the permanent strain increment $\Delta\varepsilon_p$, and the creep strain increment $\Delta\varepsilon_c$, accumulated within one temperature cycle defined by (1). In the analysis, the temperature profile applied in the TCTs was taken from the experimentally measured temperature history described in Section II. The sample was assumed to be stress-free at the bonding temperature of 250 °C, and after bonding, sufficient time was allowed at room temperature for stress relaxation prior to being subjected to the TCT shown in Fig.5.

$$\Delta\varepsilon = \frac{1}{2}\left(\varepsilon_p + \varepsilon_c\right) \quad (1)$$

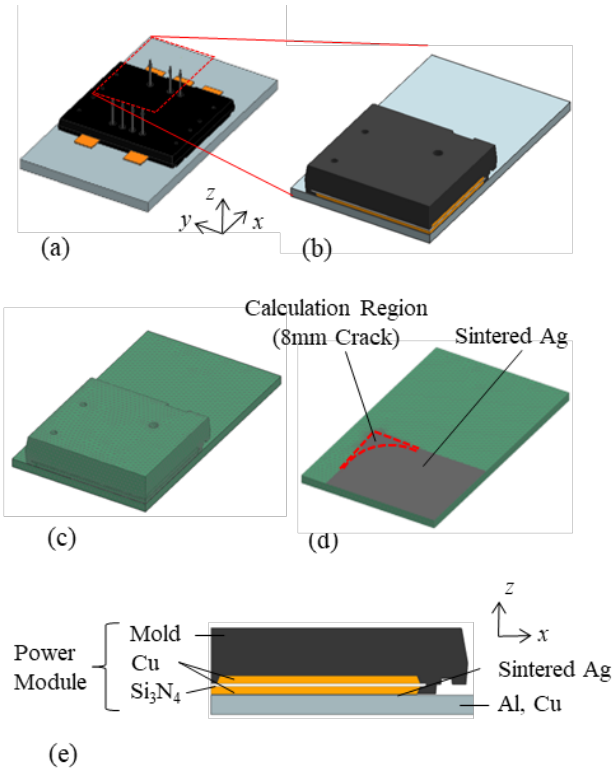


Figure 3. FEA model: (a) joint sample, (b) quarter-symmetric model, (c) overview of the mesh, (d) mesh and strain evaluation region in the sintered Ag layer, and (e) cross-sectional view of the model and material configuration.

Table 2 Mechanical properties of the materials

	Young's Modulus[GPa]	Poisson Ratio[-]	CTE [ppm/K]
Mold	12.3	0.27	13.0
Cu	129.8	0.34	16.5
Si_3N_4	330.0	0.24	4.6
Sintered Ag	Fig. 4	0.38	18.9
Al	68.6	0.33	23.6

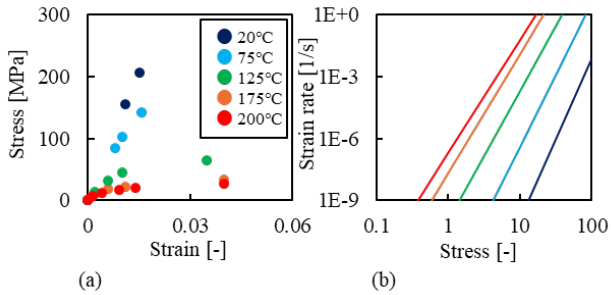


Figure 4. Material properties of sintered Ag used in the analysis obtained from three-point bending tests: (a) elastoplastic behavior and (b) creep behavior

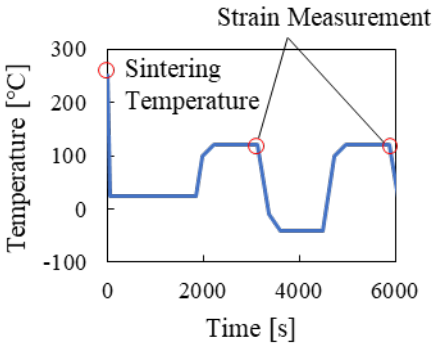


Figure 5. Temperature profile used in the analysis, corresponding to the experimental TCT condition.

IV. Results and Discussion

Figure 6 shows the relationship between the experimentally obtained lifetime, defined as the number of temperature cycles required for a crack to propagate 8 mm from the joint corner, and the analytically calculated strain amplitude Δε. The results indicate a clear and strong correlation between crack propagation lifetime and strain amplitude. Based on this relationship, a crack propagation prediction model was formulated using a Coffin–Manson-type power law [14],[15], expressed as (2)

$$N = C(\Delta\varepsilon)^{-n} \tag{2}$$

where N is the lifetime in cycles, $\Delta\varepsilon$ is the strain amplitude, and $C = 1.59$ and $n = 1.59$ are material constants determined by fitting the experimental data. The coefficient of determination for the fitted relationship exceeded $R^2 = 0.97$, demonstrating that crack propagation in large-area sintered Ag joints can be predicted with high accuracy using the strain amplitude obtained from FEA. Importantly, this result indicates that the lifetime can be consistently predicted using a single strain-amplitude parameter, even across different joint configurations and temperature cycling conditions. In other words, despite variations in bonding structures and thermal loading profiles, the crack propagation behavior can be unified and evaluated through strain amplitude derived from thermomechanical analysis. Furthermore, as shown in Fig. 6, samples No. 9, 6, 5 and 4 as shown in Table 1 exhibit relatively smaller strain amplitudes and correspondingly longer lifetimes compared with the other configurations. These observations provide important insight into the structural factors governing crack propagation behavior. Specifically, the results suggest that the lifetime of large-area sintered Ag joints can be significantly extended by reducing thermomechanical mismatch and structural constraint within the bonding configuration. In particular, a smaller difference in the coefficients of thermal expansion (CTE) between the materials adjacent to the sintered Ag layer contributes to reducing thermally induced deformation. In addition, a thinner metal plate representing the cooler reduces bending constraint, while a thicker sintered Ag layer allows for greater strain accommodation.

As a result, these structural factors effectively reduce the strain amplitude in the joint layer, leading to enhanced resistance to crack propagation during TCTs. This interpretation provides a clear design guideline.

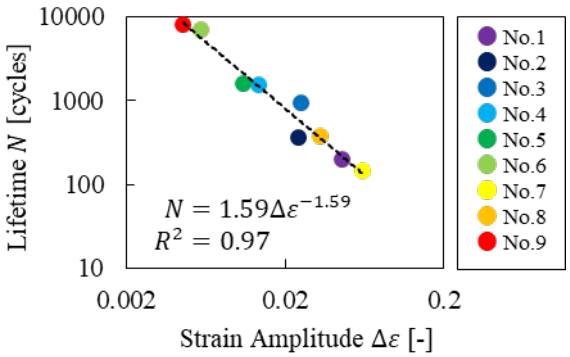


Figure 6. Relationship between crack-propagation lifetime and strain amplitude derived from FEA, including the fitted Coffin–Manson-type prediction model.

V. Application to Inverter Bonding-Structure Design

A. Design concepts

Based on the crack propagation model in the previous section, three cooler structures were designed for a three-phase inverter application, as shown in Fig. 7. The design concepts are summarized as follows:

Design 1: Standard cooler structure

Design 2: Reduced-thickness cooler

Design 3: Reduced-thickness cooler with a Cu/Al clad bonding surface

These designs were selected to systematically evaluate the effects of cooler thickness and CTE, which were identified as the dominant factors influencing the strain amplitude and crack-propagation behavior. In contrast, the thickness of the sintered Ag layer can be relatively easily adjusted in the manufacturing process, therefore, lifetime improvement was primarily pursued through the design optimization of the cooler structure.

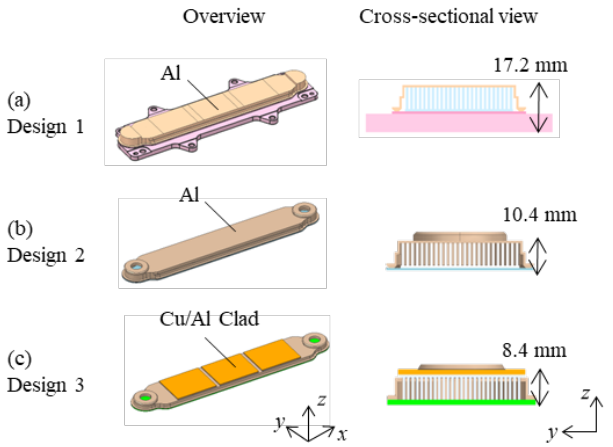
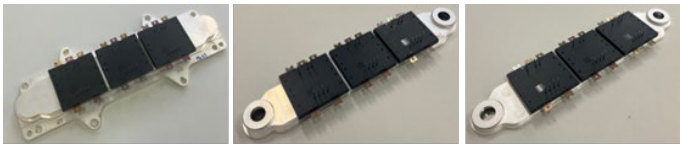


Figure 7. Three cooler designs to reduce strain amplitude : (a) standard cooler structure, (b) reduced-thickness cooler, and (c) reduced-thickness cooler with a Cu/Al clad bonding surface

B. Manufacturing prototypes

Three types of coolers designed to reduce strain amplitude were fabricated. A three-phase inverter structure was then constructed by bonding three single-phase power modules onto each fabricated cooler using sintered Ag joints shown in Fig.8. The bonding process conditions were identical to those used for the joint samples: 250 °C, 15 MPa and 15 min in an atmospheric environment .



(a) Design 1 (b) Design 2 (c) Design 3

Figure 8. Fabricated three-phase inverter prototypes: (a) Design 1, (b) Design 2, and (c) Design 3.

C. Evaluation Results

The fabricated prototypes were subjected to TCTs to evaluate crack propagation behavior in the Ag sinter layer. Crack propagation was evaluated for the module located at the edge shown in Fig.9(a), where the thermally induced stress is expected to be the highest. In the prototype structures, the distance to the Ag sinter layer was too large to allow observation by SAT. Therefore, crack propagation was evaluated by cross-sectional observation, as shown in Fig. 9(b). The crack length was defined as the average value measured at the four corners of the joint. In addition, samples were destructively inspected at each cycle count to obtain cross-sectional images. Due to limitations in the number of available prototypes, crack propagation lengths for Design 1 were obtained at 100, 250, 500, and 1000 cycles, whereas those for Design 2 and Design 3 were evaluated at 500 and 1000 cycles only.

The measurement results of crack propagation lengths are summarized in Fig. 9(c). For all three structures, the crack propagation length remained below 8 mm; however, a clear decreasing trend is observed in the order of Design 1, Design 2, and Design 3, indicating improved resistance to crack propagation.

These results demonstrate that the design modifications aimed at reducing strain amplitude are effective in suppressing crack propagation. In addition, strain amplitude analysis of the three-phase inverter structures revealed that, relative to Design 1, the strain amplitude was reduced by 46% in Design 2 and by 80% in Design 3, respectively. Furthermore, the experimental results obtained from the actual inverter prototypes validate the findings presented in Section IV, confirming that reducing strain amplitude through bonding-structure design leads to extended lifetime in practical applications.

VI. Conclusion

In this study, a design-oriented crack-propagation prediction methodology for large-area sintered Ag joints used in power module–to–cooler bonding was established.

A strong correlation between crack-propagation lifetime and strain amplitude, including both plastic and creep components, was demonstrated through TCTs and FEA. A Coffin–Manson-type relationship with high accuracy ($R^2 > 0.97$) was established, indicating that crack propagation in large-area sintered Ag joints can be quantitatively predicted using a single strain-amplitude parameter. Importantly, this result demonstrates that crack-propagation behavior can be consistently unified and evaluated across different bonding structures and TCT conditions using strain amplitude derived from thermomechanical analysis. This provides a physically interpretable and practical design guideline for reliability improvement. Based on the proposed model, three inverter cooling structures were designed and experimentally evaluated. The results confirmed that reducing strain amplitude effectively suppresses crack propagation in the sintered Ag layer, validating the applicability of the proposed methodology to actual inverter structures.

The proposed approach enables efficient and quantitative reliability assessment without extensive prototyping and provides a practical framework for the design of high-power-density and highly reliable EV inverter systems.

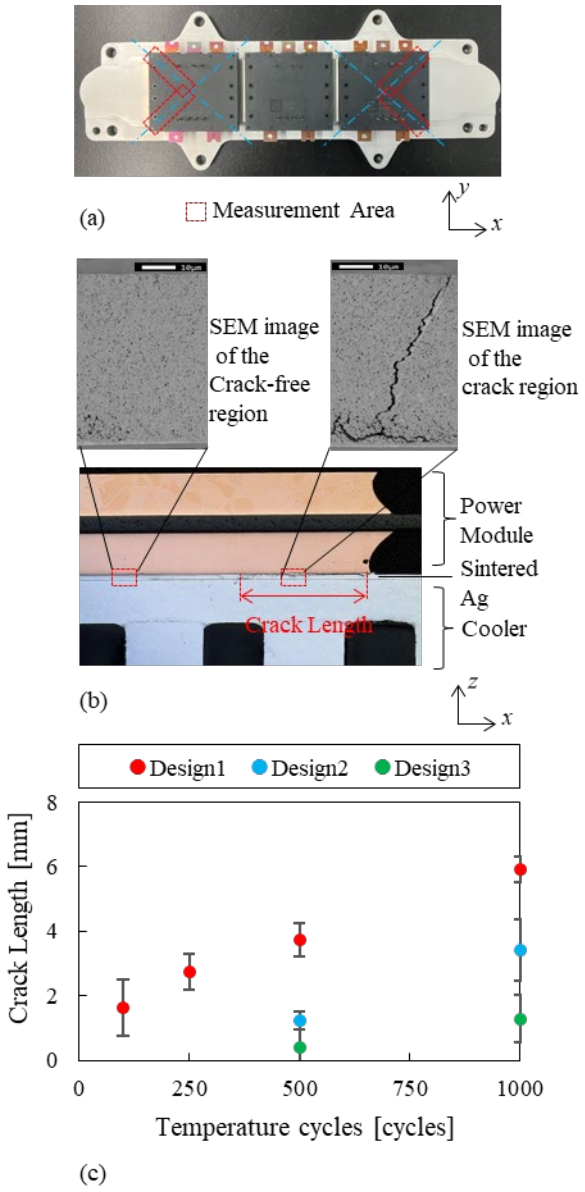


Figure 9. Evaluation of crack propagation in the sintered Ag layer of inverter prototypes: (a) evaluated edge module, (b) cross-sectional observation method, and (c) measured crack propagation lengths for each design (N ≥ 4, mean ± SD).

References

[1] T. Orville *et al.,* "Enhancing thermal efficiency in power electronics: A review of advanced materials and cooling methods," Thermo, vol. 5, no. 3, 2025.

[2] M. Schulz, S. T. Allen, and W. Pohl, "The crucial influence of thermal interface material in power electronic design, in Proc. SEMI-THERM Symp., 2013.

[3] J. Li *et al.,* "Thermal Resistance Analysis of Sn–Bi Solder Paste Used as Thermal Interface Material for Power Electronics Applications," J. Electron. Packag., vol. 136, no. 1, 2014.

[4] J. Y. So, Y. D. Yoon, and S. W. Yoon, "Thermal analysis of indirect double-sided cooling power modules considering the impact of thermal interface material characteristics," Journal of Semiconductor Technology and Science, vol. 25, no. 2, pp. 148–153, 2025.

[5] K. M. Razeeb, *et al.,* "Present and future thermal interface materials for electronic devices," Microelectron, vol.63, 2017.

[6] G. Han et *al.,* "Thermal Management of Wide-Bandgap Power Semiconductors: Strategies and Challenges in SiC and GaN Power Devices", Electronics, vol. 14, no. 21, 2025.

[7] H. Kang *et al.,* "Low Melting Temperature Sn-Bi Solder : Effect of Alloying and Nanoparticle Addition on the Microstructural, Thermal, Interfacial Bonding, and Mechanical Characteristics", Metals, vol. 11, no. 2, 2021.

[8] F. Arabi *et al.,* "Thermo-mechanical assessment of silver sintering for attaching power components," Microelectronics Reliability, vol. 114, p. 113900, 2020.

[9] K. Suganuma *et al.,* "Die-attach technology using nanosilver paste for power device applications,"
IEEE Transactions on Components and Packaging Technologies, vol. 33, no. 1, pp. 48–56, 2010.

[10] P. Paret *et al.,* "Reliability and lifetime prediction model of sintered silver under high-temperature cycling," IEEE Transactions on Device and Materials Reliability, vol. 10, issue. 5, pp. 5181-5191, 2022.

[11] MatWeb, LLC, "Material Property Data," Available: http://www.matweb.com (accessed 2024).

[12] X. Long *et al.,* "Constitutive, creep, and fatigue behavior of sintered Ag for finite element simulation of mechanical reliability: A critical review," Journal of Materials Science: Materials in Electronics, vol. 33, pp. 2293–2309, 2022.

[13] C. Chen *et al.,* "Fatigue and creep properties of sintered Ag paste from room temperature to high temperature," in TMS Annual Meeting Supplemental Proceedings, 2020.

[14] L. F. Coffin, "A study of the effects of cyclic thermal stresses on a ductile metal," Transactions of the ASME, 1954.

[15] W. Zhuang and N. Swansson, "Thermo-mechanical fatigue life prediction: A critical review," DSTO Technical Report, 1998.